Resonance Raman Spectroscopy of Nitrile Hydratase, a Novel Iron−Sulfur Enzyme†

Bridget A. Brennan, John G. Cummings, D. Bruce Chase, Ivan M. Turner, Jr., and Mark J. Nelson*

Central Research and Development, E. I. du Pont de Nemours & Company, Wilmington, Delaware 19880-0328

Received January 23, 1996; Revised Manuscript Received April 15, 1996⊗

ABSTRACT: Resonance Raman spectra of *Rhodococcus* sp. R312 (formerly *Brevibacterium* sp. R312) nitrile hydratase, a novel non-heme iron enzyme, have a large number of peaks in the 300−500 cm^{-1} region; observation of shifts in these peaks after labeling with ^{34}S shows that they arise from cysteine coordinated to the ferric ion in the protein. The rich Raman spectra result from coupling of the Fe−S stretch with cysteine side chain deformation modes; the observation of ^{15}N isotope shifts in most of these peaks suggests participation of N-donor metal ligands and peptide backbone amide nitrogens in these modes as well. The aggregate ^{34}S isotope shift is too large to result from a single cysteine ligand, consistent with the analysis of EXAFS data that shows two or three S-donor ligands [Scarrow et al. (1996) *Biochemistry 35*, 10078−10088]. Widespread ^{2}H isotope shifts seen after exchange of the protein into $^{2}H_2O$ suggest the presence of hydrogen bonds to the coordinated cysteine sulfurs. Comparison of the resonance Raman spectra of nitrile hydratase prepared at pH 7.3 and 9.0 shows a shift of intensity into the higher-energy peaks in the spectra of the latter sample. This is interpreted as resulting from an increase in Fe−S bond strength at the higher pH and is supported by observation of a small decrease in Fe−S bond length in the EXAFS analysis [Scarrow et al. (1996) *Biochemistry 35*, 10078−10088]. Such a decrease in Fe−S bond length is also consistent with pH dependent changes in EPR spectra and could reflect the loss of one or more hydrogen bonds to sulfur ligands.

Nitrile hydratases are bacterial metalloenzymes that catalyze the hydration of nitriles to amides (Nagasawa & Yamada, 1989). The enzymes from *Brevibacterium* sp. R312 [now *Rhodococcus* sp. R312 (Briand et al., 1994)] and *Pseudomonas chlororaphis* (Nagasawa et al., 1986, 1987) have been purified and shown to be non-heme iron enzymes, while the ones from *Rhodococcus rhodochrous* J1 contain non-corrinoid cobalt (Nagasawa et al., 1988, 1991). Nitrile hydratase from *Rhodococcus* sp. R312, which is very similar if not identical to the nitrile hydratase from *Rhodococcus* sp. N-774 (Mayaux et al., 1990), has two identical low-spin ferric ions per $\alpha_2\beta_2$ tetramer (94 000 Da) (Sugiura et al., 1987); these recently have been shown to be in a biologically unusual octahedral ligand field of two cysteine thiolates, a hydroxide, and three N-donor ligands, probably histidine imidazoles (Figure 1) (Nelson et al., 1991; Jin et al., 1993; Doan et al., 1996; Scarrow et al., 1996). Two other non-heme iron proteins, desulfoferredoxin and neelaredoxin, are also thought to contain mononuclear non-heme Fe^{3+} with a mixed histidine-cysteine coordination environment (Chen et al., 1994; Tavares et al., 1994).

Resonance Raman spectroscopy has proven to be an extremely useful tool for the exploration of the active sites of metallosulfur enzymes where the enzyme exhibits a S → M^{n+} charge transfer band (Spiro & Czernuszewicz, 1995). In particular, the blue copper and iron−sulfur proteins have been intensively studied by this technique (Loehr, 1992). Raman spectra of these proteins exhibit resonance-enhanced features in the 300−500 cm^{-1} region arising from the M−S stretch. In many cases, coupling between that vibration and the vibrations of the cysteine side chain(s) gives rise to a large number of peaks in that portion of the spectrum. Attempts to understand these spectra in detail have spawned elegant model studies (Han et al., 1989; Czernuszewicz et al., 1994; Qiu et al., 1994), from which it may be concluded that the energy, number, and relative intensity of the bands depend on the strength of the M−S bond and the conformation of the cysteine side chain. In addition, the effects of hydrogen bonding to the cysteines in these proteins can be revealed by resonance Raman spectroscopy of samples exchanged into $^{2}H_2O$ (Mino et al., 1987).

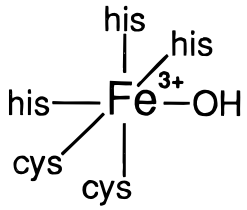

FIGURE 1: Model for the iron site in nitrile hydratase.

Nitrile hydratase prepared at pH 7.3 shows a strong absorption at 715 nm [$\epsilon \approx 1100$ $M(Fe)^{-1}$ cm^{-1}] (Nagasawa et al., 1986; Nelson et al., 1991). Excitation into that band yields an extremely well-resolved resonance Raman spectrum with evidence of at least 13 bands between 200 and 800 cm^{-1}. The similarity of this spectrum to those of the blue copper proteins was taken as strong evidence for at least one cysteine thiolate ligand to the metal ion (Nelson et al., 1991). We have obtained resonance Raman spectra of samples of nitrile hydratase enriched with ^{34}S and ^{15}N and

† Contribution 7320 from Central Research and Development.

* Please address communications to Mark J. Nelson. Phone: 302-695-4124. Fax: 302-695-4260. E-mail: NELSONMJ@ESVAX.DNET.DUPONT.COM.

⊗ Abstract published in *Advance ACS Abstracts,* July 1, 1996.

[1] Abbreviations: BHK buffer, 0.1 M HEPES with 0.04 M sodium butyrate at pH 7.3 (4 °C); CCD, charge-coupled device; ENDOR, electron nuclear double resonance; EXAFS, extended X-ray absorption fine structure; HEPES, *N*-(2-hydroxyethyl)piperazine-*N*′-2-ethanesulfonic acid; XANES, X-ray absorption near-edge spectroscopy.

S0006-2960(96)00163-8 CCC: $12.00

exchanged into ^2H_2O or $H_2{}^{18}O$, prepared at both pH 7.3 and 9.0. Our goal is to develop resonance Raman spectroscopy as a complement to EPR, electron nuclear double resonance (ENDOR),[1] and extended X-ray absorption fine structure (EXAFS) spectroscopies in probing the effects of substrates and inhibitors on the metal site of the enzyme.

MATERIALS AND METHODS

Culture Conditions. *Rhodococcus* sp. R312 strain A4 (Technische Universiteit Delft, LMD#79.2), an amidase-deficient mutant, was cultured by an adaptation of Bernet et al. (1990). For cultures up to 1 L, the culture medium comprises 50 mM K_2HPO_4, pH 7.2, 36 μM Fe (added as a solution of 0.10 M $FeSO_4$ and 0.5 M citric acid at pH 6.5), 44 μM thiamine hydrochloride, 2.0 mM $MgSO_4$, 75 mM NH_4Cl, 1% (w/v) dextrose, 0.2% (v/v) acetonitrile, and 20% (v/v) trace element solution consisting of 0.8% (v/v) concentrated HCl, 6 mM Fe (added as the ferric citrate solution), 1.5 mM $MnCl_2$, 0.38 mM $NiSO_4$, 0.40 mM $CuSO_4$, 0.43 mM $ZnSO_4$, 1.6 mM H_3BO_3, 0.18 mM $NaMoO_4$, 0.12 mM KI, and 0.16 mM KBr. Fifteen milliliters of this culture was used to inoculate a 2 L shake flask containing 1 L of this media.

The 1 L culture was used to inoculate a 40 L New Brunswick Scientific Mobile Pilot Plant fermentor containing 30 L of culture media with the following modifications: 1 mL of the trace metals solution, 50 μM Fe (as ferric citrate), 150 mM NH_4Cl, 5.7 mM NaCl, 10 mL of antifoam (Mazu DF 204; PPG Industries), and 75 mL of acetonitrile. The 30 L culture was used to inoculate a 400 L New Brunswick Scientific Fermentation System containing 270 L of media with the following further modifications: 18 mM K_2HPO_4, pH 7.2, and 70 mM $(NH_4)_2SO_4$ (instead of NH_4Cl). The pH was maintained automatically at 7.0 by addition of 50% NH_4OH solution or concentrated H_3PO_4. The growth was monitored turbidometrically, and the culture was harvested at $OD_{660} \approx 8-10$ (approximately 25−30 h after inoculation). Cells were obtained by centrifugation, and the paste was frozen as pellets in liquid nitrogen. Yields were about 8 g (wet weight) of cell paste per liter. Frozen cell paste was stored at −80 °C.

Growth on ^{15}N. Cells were grown in the 40 L fermentor using 4 mM $^{15}NH_4Cl$ (99.9% enriched; Isotec) as the sole source of nitrogen and no acetonitrile. The culture was harvested at $OD_{660} \approx 4$ and yielded about 2.5 g (wet weight) of cell paste per liter.

Growth on ^{34}S. Cells were grown in the 40 L fermentor using culture media containing 245 mM $^{34}SO_4{}^{2-}$ prepared by heating elemental sulfur (93.9% enriched; Isotec) to 85 °C in aqua regia. Otherwise, only sulfur free reagents were used to make the culture media. The media also contained 5.3 mM $NaHCO_3$ and 2 mM $MgCl_2$ (instead of $MgSO_4$), and the ferric citrate solution was made with $Fe(NO_3)_3$. Nitrogen was supplied as 60 mM NH_4Cl and 75 mM NH_4NO_3. No trace metals solution was added. The cells were harvested at $OD_{660} \approx 6.8$; the yield was 7 g (wet weight) of cell paste per liter.

Enzyme Purification and Assay. Nitrile hydratase was purified by an adaptation of the procedure of Nagasawa et al. (1986). All steps were performed at 4 °C using 0.10 M *N*-(2-hydroxyethyl)piperazine-*N*-2-ethanesulfonic acid (HEPES) buffer with 0.04 M sodium butyrate adjusted to pH 7.0 at room temperature with KOH (BHK buffer). Fifty grams of frozen cell paste was suspended and thawed in 250 mL of BHK buffer at 4 °C and then disrupted in a Bead Beater (Biospec Products) in four to seven 1 min beatings each separated by 1.5 min, using 250 g of 0.5 mm glass beads. The chamber of the Bead Beater was immersed in a water/ice bath at 0−4 °C. The decanted cell suspension and two or three washings of the beads were combined and centrifuged for 30 min at 24000*g*.

The supernatant was decanted and brought to 40% saturation by addition of solid ammonium sulfate. The suspension was stirred for 1 h, and the precipitated proteins were removed by centrifugation for 30 min at 24000*g*. The supernatant from the 40% ammonium sulfate precipitation was applied at 15 mL/h to a Phenyl Sepharose CL-4B (Pharmacia) column (2.5 × 15 cm) equilibrated with BHK buffer, 25% saturated with ammonium sulfate. The column was washed with approximately 800 mL of this buffer until the eluent $OD_{280} \approx 0$. The column was eluted with 1 L of BHK buffer, and 5 mL fractions were collected. The fractions with the highest specific activities were pooled and dialyzed overnight against BHK buffer containing 0.1 M KCl.

The dialyzed enzyme solution was applied to a DEAE-Sephacel (Pharmacia) column (2.5 × 10 cm) equilibrated with BHK buffer containing 0.1 M KCl. The column was washed with 200−300 mL of this buffer and eluted with a 500 mL linear gradient from 0.3 to 0.6 M KCl in BHK; 5 mL fractions were collected. The fractions with the highest specific activities were pooled and brought to 25% saturation with solid ammonium sulfate. This solution was applied to a Phenyl Sepharose CL-4B column (2.5 × 15 cm) equilibrated with BHK buffer 25% saturated with ammonium sulfate. The column was washed with 200−300 mL of this buffer and eluted with a log gradient of BHK buffer from 25 to 0% saturation with ammonium sulfate; 5 mL fractions were collected. The fractions with the highest specific activities were checked for homogeneity by EPR (see Results) and separated into two pools, one containing homogeneous active protein and the other containing a mixture of forms. Typical yields are 40 mg of homogeneous active nitrile hydratase with a specific activity of 850 U/mg and 40 mg of the mixture. The purified protein was stored at 4 °C.

Nitrile hydratase activity was measured as the rate of hydration of 10 mM methacrylonitrile in 0.10 M KH_2PO_4 at pH 7.0 by following the increase in absorbance at 224 nm ($\Delta\epsilon = 3.4\ M^{-1}\ cm^{-1}$) at 25 °C. One unit of activity is defined as 1 μmol of methacrylamide produced per minute and corresponds approximately to 2 U as measured by the hydration of propionitrile. Protein was estimated using $\epsilon_{280} = 1.22\ (mg/mL)^{-1}\ cm^{-1}$ (Nagasawa et al., 1986).

Sample Preparation. Protein solutions were concentrated using Amicon Centriprep 10 and Centricon 10 devices. The high-pH form of nitrile hydratase was prepared from the heterogeneous pool of protein by dialysis against 0.050 M sodium borate and 0.040 M sodium butyrate at pH 9.0 for 2−3 days. The homogeneity of the sample was assessed by EPR. Samples were prepared in ^2H_2O by dialysis against buffer prepared in ^2H_2O for 2−3 days, while the control sample was dialyzed against natural abundance buffer. Samples to be prepared in $H_2{}^{18}O$ were concentrated, then lyophilized, and reconstituted with $H_2{}^{18}O$ (95% enriched,

Aldrich); again a control sample was reconstituted with natural abundance deionized water. Samples in labeled water and natural abundance controls were checked for activity and pH, and EPR spectra were obtained before use. These agreed satisfactorily.

Resonance Raman Spectroscopy. The sample holder was cooled using an Air Products LT3-110 cryostat using liquid nitrogen as the refrigerant with a typical sample temperature of 80 K. Samples were loaded onto a precooled (270 K) gold-plated copper cold finger with wells for four 12 μL samples. The samples were frozen rapidly; Dewar evacuation was begun at a sample temperature of 200 K to minimize the possibility of lyophilization. Samples of isotopically labeled and natural abundance materials were loaded in pairs, and all isotope shifts were referenced to a spectrum of natural abundance protein obtained immediately before or after the spectrum of the labeled sample, with no alteration of calibration or excitation wavelength.

A Spectra-Physics 2040 Ar-ion laser was used at 514 nm to pump a Spectra-Physics 3900 Ti-sapphire laser capable of producing several hundred milliwatts of tunable radiation from 680 to 760 nm. The output of the Ti-sapphire laser was optically filtered to remove nonlasing emission using a double-pass prism monochromator followed by a Newport Model 910 spatial filter. Power at the sample was typically 50 mW. Raman spectra were recorded in a 180° backscattering configuration using an f/1.3 camera lens for collection. The collected Raman-scattered light was dispersed using a SPEX Model 1877 triplemate monochromator and detected with a Tektronix 1024 × 1024 thinned, backside-illuminated charge-coupled device (CCD) element (peak quantum efficiency of 90% at 700 nm) mounted in a Photometrics CCD9000 detection system. The CCD was operated at −110 °C. The spectrometer was calibrated using the atomic emission lines from Ar, Kr, Ne, or Xe pen lamps. Spectral resolution was 4−6 cm^{-1}, corresponding to 5−7 pixels on the CCD. The data were processed and displayed using Labcalc (Galactic Industries).

We used a 600 groove/mm grating to disperse the collected light over approximately 800 cm^{-1}, giving ca. 0.8 cm^{-1}/pixel. The average width of the peaks in the spectrum was 12 cm^{-1}; thus, the line shape of each peak was defined by about 15 pixels. This was sufficient to yield peak positions in spectra obtained on the same day that agreed to within ≤0.5 cm^{-1}. Spectra taken on different days were consistent as to number of peaks and relative intensities and line shapes, but the absolute frequencies varied by as much as 3 cm^{-1}. Therefore, isotope shifts were measured using spectra taken on the same day without recalibration of the spectrometer. Comparison of multiple measurements of the isotope shifts generally yielded standard deviations of the mean of ≤0.6 cm^{-1}.

EPR Spectroscopy. EPR spectra were obtained using a Brucker EM-200 spectrometer with an Oxford Instruments ESR900 liquid helium cryostat. The conditions were as follows: microwave frequency, 9.4 GHz; modulation amplitude, 1.0 mT; microwave power, 2 mW; *T*, 20 K; and scan rate, 0.48 mT/s.

RESULTS

The buffers used for the purification and sample preparation of nitrile hydratase contain 40 mM butyrate to maintain enzyme activity (Nagasawa et al., 1986). We have recently shown that butyrate is a competitive inhibitor of nitrile hydratase from *Rhodococcus* sp. R312, with $K_I = 2$ mM at pH 7 (J. G. Cummings, unpublished). Consequently, the samples studied in this and previous work (Sugiura et al., 1987; Nelson et al., 1991; Jin et al., 1993) represent a "butyrate-inhibited" form of nitrile hydratase. Even when butyrate is used, the purified enzyme can be a mixture of species. The dominant form at pH 7.3 is characterized by the EPR (g_1, g_2, and $g_3 = 2.27$, 2.14, and 1.97, respectively) and visible ($\lambda_{max} \approx 715$ nm) spectra already published (Figures 2a and 3a) (Nagasawa et al., 1986; Sugiura et al., 1987). This form of the enzyme shows nitrile-hydrating activity when diluted into assay buffer prepared without butyrate. The second form shows different EPR (g_1, g_2, and $g_3 = 2.20$, 2.12, and 1.99, respectively) and visible ($\lambda_{max} \approx$ 690 nm) spectra (Figures 2b and 3b) and may be prepared deliberately by dialysis of active enzyme into pH 9 buffer. When diluted into assay buffer prepared without butyrate, this form shows no nitrile-hydrating activity. We shall refer to these as "low-pH" and "high-pH" forms of nitrile hydratase. The EPR spectrum of the high-pH form is similar to that of the "substrate-bound" form (Sugiura et al., 1987), and its visible spectrum is similar to that of a butyrate-free active form that was prepared at pH 7 (Honda et al., 1994).

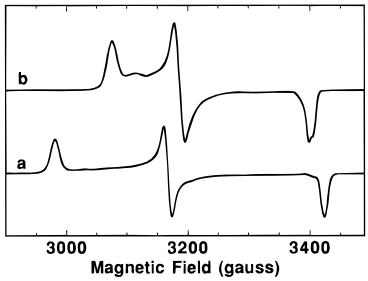

FIGURE 2: EPR spectra of nitrile hydratase: (a) pH 7.3 and (b) pH 9.0.

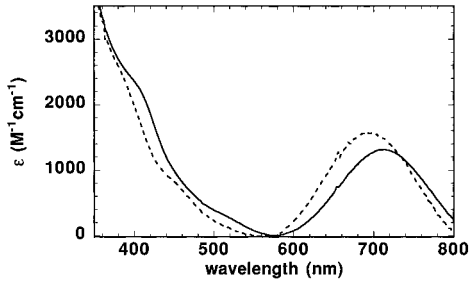

FIGURE 3: Visible spectra of nitrile hydratase: (a) pH 7.3 (—) and (b) pH 9.0 (- - -).

Analysis of the EPR spectra of the low- and high-pH forms allows calculation of the relative splittings among the d_{xy}, d_{xz}, and d_{yz} orbitals of the low-spin ferric ions in the protein (Taylor, 1977). This analysis assumes no covalency in the metal−ligand bonds, which is inconsistent with the proposed model for the iron site structure (Figure 1). However, EXAFS (Scarrow et al., 1996) studies show that the ligands are the same in both forms, so it is reasonable to assume that the orbital reduction factors resulting from covalent metal−ligand interactions are approximately the same. In that case, the analysis is useful for comparison. In both the low-pH and high-pH forms, the ground state electronic configuration is predicted to be $d_{yz}^2\, d_{xz}^2\, d_{xy}^1$, but in the high-pH form of the enzyme, the EPR analysis predicts that the d_{xy} orbital is significantly higher in energy.

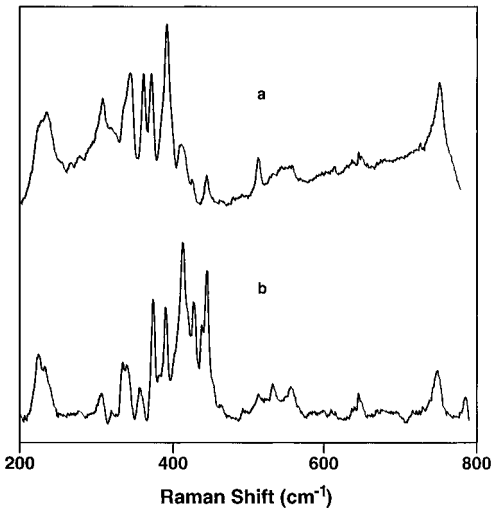

FIGURE 4: Resonance Raman spectra of nitrile hydratase obtained with 714 nm excitation: (a) pH 7.3 and (b) pH 9.0.

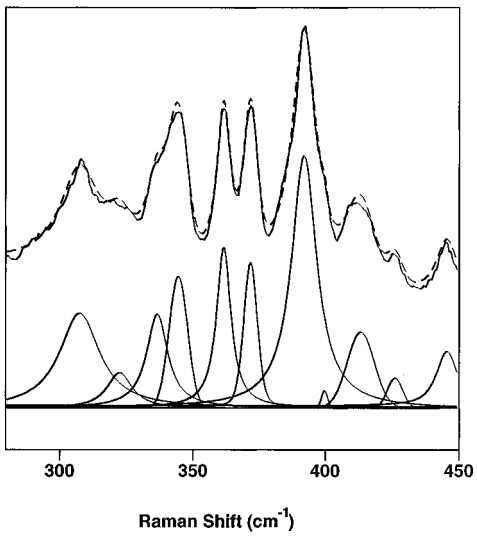

FIGURE 5: Resonance Raman spectra of nitrile hydratase at pH 7.3: upper, (—) data and (- - -) fit using a mixture of Gaussian and Lorentzian line shapes; and lower, individual peaks from the deconvolution.

Resonance Raman Spectroscopy of the Low-pH Form of Nitrile Hydratase. Figure 4a shows the resonance Raman spectrum of nitrile hydratase prepared at pH 7.3, obtained with 714 nm excitation. This spectrum shows substantially higher resolution than the spectrum previously published (Nelson et al., 1991), primarily as the result of improved sample preparation (to remove the contaminating high-pH form), low-temperature data acquisition, excitation directly into the charge transfer band, and use of more sensitive Raman detection equipment.

The spectra were deconvoluted into a set of peaks that were allowed to have a mixture of Gaussian and Lorentzian line shapes (Figure 5, Table 1). All of the peaks in the 200−800 cm^{-1} region are assigned to the protein chromophore with the exception of the two ice bands at 227 and 310 cm^{-1}. There are no features outside of this region attributable to the protein; in particular, there are no peaks in the 1100−2000 cm^{-1} region as would be expected were tyrosine phenoxide or nitric oxide coordinated to the iron (Que & Heistand, 1979; Benko & Yu, 1983; Carrano et al., 1990; Brown et al., 1995). This rich resonance Raman spectrum is highly reminiscent of those of proteins with cysteine coordinated to a metal ion, in which the large number of peaks in this region is thought to result from mixing between the metal−sulfur stretching interaction and cysteine side chain deformations (Loehr, 1992; Spiro & Czernuszewicz, 1995).

Table 1: Observed Raman Frequencies and Isotope Shifts (cm^{-1}) for Nitrile Hydratase in the Low- and High-pH Forms[a]

low-pH form				high-pH form		
$\Delta\nu$	$\Delta(\Delta\nu)^{34}S$	$\Delta(\Delta\nu)^{15}N$	$\Delta(\Delta\nu)^{2}H_2O$	$\Delta\nu$	$\Delta(\Delta\nu)^{34}S$	$\Delta(\Delta\nu)^{2}H_2O$
238	−2.0	−1.4	−1.6	235	−0.4	−2.6
326	−1.4	*b*	−0.6	320	−2.1	0.7
337	−1.9	−7.1	0.6	333	−0.6	0.2
345	−2.1	−3.7	−0.5	341	−0.7	−1.5
363	−1.1	−0.8	−1.6	357	−1.4	−0.9
373	−0.8	−1.4	−0.4	374	−0.1	−1.9
b				383	−0.1	0.3
393	−2.4	−2.0	−0.6	390	−0.7	−0.2
401	−0.5	*b*	−1.0	404	0.7	1.1
413	−0.8	−2.1	0	413	−0.2	−2.5
b				420	0.1	0.3
427	0	0	−0.2	428	−0.3	−1.4
b				438	−0.7	−1.8
446	−1.7	−4.8	−0.2	445	−0.9	−8.6
b				454	0.1	0.6
b				465	0.2	−1.6
515	−3.3	0.2	1.0	*c*		
752	−3.4	−2.1	−0.7	749	−3.0	−0.7

[a] The precision in the absolute frequencies is approximately ±2 cm^{-1}, and the standard deviation in multiple measurements of the isotope shifts is ≤0.6 cm^{-1}. [b] Not observed. [c] Overlap and low signal-to-noise prevented deconvolution.

In order to determine whether a similar mechanism is responsible for the nitrile hydratase spectrum, we grew *Rhodococcus* sp. 312 using $^{34}SO_4^{2-}$ as the sole sulfur source and purified the protein as before. Comparison of the resonance Raman spectra of the ^{34}S-enriched and natural abundance nitrile hydratases shows shifts of up to −3.4 cm^{-1} in the positions of the peaks (Table 1). The largest shifts are observed in the features at 345, 393, 515, and 752 cm^{-1}. All of the other peaks have observable shifts with the exception of the feature at 427 cm^{-1}.

No single ^{34}S shift is as large as that predicted by a model of an isolated Fe−S two-body oscillator, approximately −8 cm^{-1} for ν_{Fe-S} at 400 cm^{-1}. This is similar to what is seen in the resonance Raman spectra of the blue copper proteins azurin and plastocyanin, where the largest ^{34}S isotope shifts are −3.8 and −2.3 cm^{-1}, respectively, although a simple two-body Cu−S model predicts a shift of −7.7 cm^{-1} (Dave et al., 1993; Andrew et al., 1994; Qiu et al., 1995). This is consistent with coupling of the metal−sulfur stretch to the deformation modes of the cysteine side chains that distributes the ^{34}S isotope shift among all of the bands with ν_{M-S} character. The distribution of the ^{34}S isotope shift among most of the peaks in the spectrum of nitrile hydratase suggests that the conformation of the cysteine side chains is appropriate to engender mixing of a large number of states. The total of the ^{34}S shifts of the deconvoluted peaks in the 300−500 cm^{-1} region is −12.7 cm^{-1}, almost twice that predicted for a single two-body Fe−S oscillator at 400 cm^{-1}. This shows that these features cannot arise from a single Fe−S interaction; thus, the spectrum either comprises the overlaid spectra of two different (isolated) Fe−S systems or represents the coupled vibrations of a site with more than one Fe−S bond.

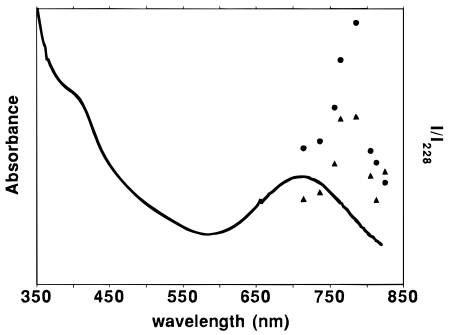

FIGURE 6: Excitation profiles of the resonance Raman spectra of nitrile hydratase at pH 7.3: (▲) 345 cm^{-1} peak and (●) 393 cm^{-1} peak.

Overall, the largest ^{34}S isotope shift seen in the nitrile hydratase spectrum is the -3.4 cm^{-1} shift of the feature at 752 cm^{-1}. A feature at similar energy is observed for other metal−cysteinate proteins and has been assigned to a C−S mode that is enhanced by coupling to the M−S stretching modes (Andrew et al., 1994). The calculated ^{34}S shift for a two-body C−S oscillator is -6 cm^{-1}.

Resonance Raman spectra of nitrile hydratase purified from bacteria grown using $^{15}NH_4^+$ as the sole nitrogen source also show shifts in most of the features between 300 and 500 cm^{-1} (Table 1). This implies involvement of modes involving N-donor metal ligands and peptide amide nitrogens in these vibrations. In addition, the feature at 238 cm^{-1} shows a ^{15}N isotope shift of -1.4 cm^{-1}, consistent with it representing an Fe−imidazole stretch (see below).

Exchange of the protein into buffer prepared with ^2H_2O yields a spectrum with numerous small shifts in the peaks. The shifts in the peaks in the 300−500 cm^{-1} region (Table 1) are much smaller than would be expected for a resonance-enhanced vibration due to a coordinated hydroxide.[2] In addition, the lack of significant ^{18}O isotope shifts in spectra of protein lyophilized and reconstituted into $H_2{}^{18}O$ (data not shown) suggests that the Fe−O stretching vibration of the coordinated hydroxide is not coupled to the S → Fe charge transfer absorption band and that none of the peaks in the Raman spectrum may be attributed to an Fe−O vibration.

Figure 6 shows representative excitation profiles for two bands in the resonance Raman spectrum of the low-pH form of nitrile hydratase. The strongest features are still observable when the excitation wavelength is more than 100 nm above the peak of the absorption. Unfortunately, use of excitation wavelengths shorter than 700 nm resulted in large fluorescence backgrounds, limiting the spectral width of the excitation profile on the high-energy side of the peak. These data establish that the observed Raman features arise from vibronic coupling to the long-wavelength absorption band. The sulfur isotope data confirm that this absorption has substantial cysteine sulfur to iron charge transfer character.

Resonance Raman Spectroscopy of the High-pH Form of Nitrile Hydratase. The resonance Raman spectrum of this form of nitrile hydratase is shown in Figure 4b. These samples are significantly more fluorescent than those of the low-pH form, somewhat inhibiting data collection. Deconvolution of these spectra yielded 15 peaks in the 300−500 cm^{-1} region (Figure 7, Table 1). Although the energies of the vibrations in the low- and high-pH forms are very similar, the intensities of the individual peaks are substantially different, with the more intense features at higher energy in the spectrum of the high-pH form. Specifically, the strong peak at 393 cm^{-1} in the spectrum of the low-pH form is no longer the dominant spectral feature, the sharp peak at 363 cm^{-1} nearly disappears, and the strong multiplet with features at 337 and 345 cm^{-1} is greatly diminished. The relative intensities of the 413 and 445 cm^{-1} features are greatly increased in the spectrum of the high-pH form. There is much less resolution in the features around 515 cm^{-1} in the spectra of the high-pH form, but the feature corresponding to ν_{C-S} is still observable at 749 cm^{-1}.

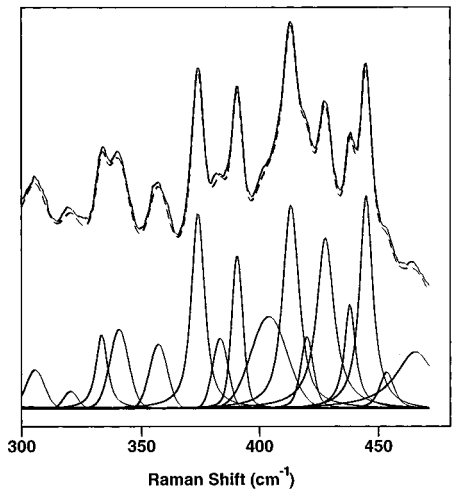

FIGURE 7: Resonance Raman spectra of nitrile hydratase at pH 9.0: upper, (—) data and (- - -) fit using a mixture of Gaussian and Lorentzian line shapes; and lower, individual peaks from the deconvolution.

Spectra of the high-pH form of nitrile hydratase enriched with ^{34}S show small shifts in most of the deconvoluted peaks (Table 1). The largest ^{34}S isotope shift in the 300−500 cm^{-1} region is -2.1 cm^{-1} in the weak 320 cm^{-1} peak. The two largest ^{34}S isotope effects in major peaks are -1.4 cm^{-1} in the peak at 357 cm^{-1} and -0.9 cm^{-1} in the 445 cm^{-1} feature, again substantially smaller than expected on the basis of the two-body Fe−S model. As in the case of the low-pH form of the enzyme, this suggests that the intrinsic isotope shift is distributed among many modes with Fe−S character, implying mixing between Fe−S stretching and the cysteine side chain deformation modes. The sum of the ^{34}S isotope effects of the features between 300 and 500 cm^{-1} is -7.3 cm^{-1}, significantly smaller than the -12.7 cm^{-1} seen in the spectra of the low-pH form. This small aggregate ^{34}S isotope shift raises the possibility of the loss of one of the coordinated cysteines. There are three arguments against this. First, it is unlikely that such a large number of features in the resonance Raman spectrum could arise from a single iron−cysteine interaction. Second, EXAFS spectra of the low- and high-pH forms (Scarrow et al., 1996) show that the ligand field is the same in the two cases. Third, the intensity of the long-wavelength S → Fe charge transfer band is approximately the same in the low- and high-pH forms, implying an equivalent number of Fe−S interactions.

Exchange of the high-pH form into buffer prepared with ^2H_2O again yields a spectrum with numerous shifts in the peaks, some sizable (Table 1). In particular, the shifts in

[2] Treating the ligand as a single unit, a two-body analysis predicts a shift of -8.6 cm^{-1} for Fe−OH and -15.4 cm^{-1} for Fe−OH_2 at 400 cm^{-1} upon deuteration.

the 445 (-8.6 cm^{-1}) and 413 (-2.5 cm^{-1}) cm^{-1} peaks are very large compared to the solvent deuterium isotope shifts seen in spectra of blue copper proteins. The -2.6 cm^{-1} shift in the 235 cm^{-1} feature is larger than that seen in the 238 cm^{-1} feature in the spectra of the low-pH form. With the exception of the -8.6 cm^{-1} shift in the 445 cm^{-1} feature, these ^2H_2O dependent isotope shifts are much smaller than would be expected for a resonance-enhanced vibration due to a bound hydroxide. As in the case of the low-pH form, there are no significant ^{18}O isotope shifts in spectra of the high-pH form lyophilized and reconstituted into $H_2{}^{18}O$ (data not shown); in particular, the 445 cm^{-1} peak (that shows the large ^2H shift) is shifted $+1.0$ cm^{-1} upon exchange into $H_2{}^{18}O$. Again we attribute none of the peaks in the spectrum of the high-pH form to bound hydroxide.

DISCUSSION

The non-heme ferric ions in nitrile hydratase exist in a biologically novel ligand field that results in unusual physical properties, including a low-spin ($S = {}^1/_2$) electronic configuration for the iron and a strong absorbance at 715 nm [$\epsilon \approx$ 1100 M(Fe)$^{-1}$ cm^{-1}] that gives the protein a green color (Nagasawa et al., 1986; Sugiura et al., 1987). EXAFS, resonance Raman, and ENDOR studies have led to the model of the iron site shown in Figure 1 (Nelson et al., 1991; Jin et al., 1993; Doan et al., 1996; Scarrow et al., 1996). The presence of cysteine ligands to the ferric ion was suggested by the similarity of the resonance Raman spectra of nitrile hydratase to those of blue copper proteins (Nelson et al., 1991), for which the features in the low-frequency region have been assigned to Cu−cysteine modes. That suggestion was confirmed in this work by the observation of substantial ^{34}S shifts of the features in the 300−500 cm^{-1} region of resonance Raman spectra obtained with excitation into the 715 nm band. This also confirms the assignment of that absorption as one with substantial S → Fe charge transfer character.

Analysis of the Iron−Cysteine Coordination. A thorough understanding of these spectra and their implications for iron−cysteine coordination in nitrile hydratase will have to await a complete normal mode analysis that is beyond the scope of the current work. It has been difficult to attain an intuitively reasonable description of the metal−cysteine interactions from normal mode analysis of the much simpler blue copper proteins (Urushiyama & Tobari, 1990; Qiu et al., 1994). In the absence of that analysis for nitrile hydratase, we will base our discussion on the thorough exploration of blue copper proteins, ferredoxins, and the synthetic models for each that has appeared in the last decade (Loehr, 1992; Spiro & Czernuszewicz, 1995). In a recent elegant study, Spiro and colleagues explored a series of alkyl thiolate complexes of Cu^{2+} as models for the metal site in blue copper proteins (Qiu et al., 1994). They demonstrated that coupling of C−C−C and C−C−S bending modes to the metal−sulfur vibration contributes importantly to the resonance Raman spectra. Translating these results to an idealized cysteine ligand, they suggested that the $C^{\beta}-C^{\alpha}-N$, $C^{\beta}-C^{\alpha}-C(O)$, and $C^{\alpha}-C^{\beta}-S$ bending modes all mix with the metal−sulfur stretching modes via coupling through $HC^{\alpha}-C^{\beta}H$ torsional modes to yield the complicated spectra obtained from metal−cysteine proteins (Qiu et al., 1994). In the case of the blue copper proteins, the side chain of the cysteine coordinated to the copper has a nearly 180° $Cu-S-C^{\beta}-C^{\alpha}$ dihedral angle that maximizes the interactions between the Cu−S and protein modes (Han et al., 1991).

The model for the structure of the metal site in nitrile hydratase (Figure 1) differs from the sites in the blue copper proteins and synthetic models in having distorted octahedral coordination and more than one cysteine thiolate ligand. In principle, this could lead to significantly more complicated Raman spectra. That notion is borne out by the large number of peaks in the spectra in Figures 5 and 7. The increased complication can come from two sources: coupling of additional side chain modes arising from the second cysteine ligand and coupling between the two Fe−S units. The number of intense peaks in the spectra suggests that one or both cysteine side chains have a $Fe-S-C^{\beta}-C^{\alpha}$ dihedral angle similar to that found in the blue copper proteins, and appropriate to engender coupling between the side chain and Fe−S vibrational modes. Additional support for similarity in side chain conformation between the two classes of proteins comes from the observation of ^{15}N isotope shifts in the peaks in the 300−500 cm^{-1} region of the nitrile hydratase spectra. Spectra of ^{15}N-labeled plastocyanin and azurin showed shifts of up to -3.8 cm^{-1}, none of which appears to arise from the metal-coordinated imidazole (Loehr, 1992; Sanders-Loehr, 1993; Qiu et al., 1995). This evidence was interpreted as demonstrating coupling between the Cu−S stretching modes and those involving the cysteine amide nitrogen. At least some of the ^{15}N shifts we observe probably have a similar origin, but we cannot be definitive because the nitrile hydratase is uniformly ^{15}N labeled and we cannot rule out contributions from coupling between Fe−N(His) and Fe−S(Cys) modes to the ^{15}N shifts (see below).

The existence of the second Fe−S bond in nitrile hydratase also raises the possibility of coupling between the two Fe−S units. Indeed, it is intuitively unreasonable that there would be no coupling between them. For the two Fe−S motions to be uncoupled would require that the iron nucleus remain essentially motionless in any Fe−S stretching mode, so as not to couple the Fe−S stretching mode of the other cysteine. This requirement could only be met if the coordination shell of the iron were so rigid that the metal ion could not be displaced by excitation into higher Fe−S vibrational modes. Thus, whereas the features in the spectra of the blue copper proteins arise fundamentally from an isolated Cu−S vibrational mode, those in nitrile hydratase arise from S−Fe−S modes in which the two S−Fe motions must be coupled.

One could consider the S−Fe−S unit in Figure 1 to have pseudo-C_{2v} symmetry, as was proposed to explain the resonance Raman spectrum of the oxidized center II site in desulfoferredoxin (Tavares et al., 1994). This would yield two primary features, the in phase (symmetric) and out of phase (antisymmetric) stretching modes of the S−Fe−S unit. The symmetric mode should be at lower energy and substantially more intense than the antisymmetric mode. Coupling of each of these S−Fe−S modes to the cysteine side chain modes would result in splitting of these primary features into a set of daughter peaks, as discussed above. In spectra of nitrile hydratase, the intense peaks are clustered in the 300−500 cm^{-1} region. If we assign those peaks to the "symmetric" S−Fe−S stretch, it is tempting to assign the relatively weak feature at 515 cm^{-1} as one of the peaks arising from the "antisymmetric stretch", particularly in light of its large (-3.3 cm^{-1}) ^{34}S isotope shift. We attempted to explore this idea further, but it proved impossible to

deconvolute reliably the spectra in the vicinity of the 515 cm^{-1} peak because the features were too weak. We conclude that assignment of regions of the spectra to symmetric and antisymmetric S−Fe−S modes is speculative at this time.

There are substantial differences in the resonance Raman spectra of the low-pH and high-pH forms of nitrile hydratase. The Raman and EXAFS data show that there is no loss or gain of cysteine ligands upon raising the pH. As noted above, the most intense resonance Raman features move to higher energy in the spectra of the high-pH form, implying that one or both of the Fe−S bonds are stronger in the enzyme at pH 9 (den Blaauwen et al., 1993). Also, although the frequencies of the peaks that appear in both spectra are approximately the same, the magnitude of the ^{34}S isotope shifts for corresponding peaks varies substantially. A similar phenomenon is observed in spectra of the blue copper proteins, where the relative constancy of the observed frequencies is taken as evidence for conservation of the cysteine side chain conformation (Han et al., 1991). The shift in intensities of the bands is thought to result from structural differences in the copper site reflected in alteration of the coupling between the Cu−S stretching and cysteine deformation modes (Andrew et al., 1994; Dave et al., 1994; Qiu et al., 1995). By analogy, the low-pH and high-pH forms of nitrile hydratase appear to have similar conformations of the cysteine side chains as revealed by resonance Raman spectroscopy. At a qualitative level, however, there is evidence for a change in the iron site geometry that alters the coupling between the Fe−S and cysteine side chain modes. Comparison of the X-ray absorption near-edge (XANES) and EXAFS data of the two forms shows that the ligands to the iron are identical and that the dominant geometry change that gives rise to the difference in intensities observed in the Raman spectra is a shortening of the Fe−S bond in the high-pH form (Scarrow et al., 1996).

In the presence of a reliable force field, the difference in Fe−S bond lengths between the low-pH and high-pH forms of nitrile hydratase could be measured. Again, a complete normal mode analysis is beyond the scope of the current work. At this stage of our analysis, we will estimate the difference by the use of Badger's rule (Badger, 1934; Herschbach & Laurik, 1961), making assumptions about the "native" frequency of the Fe−S stretch in each case. The most intense peak in the spectra of the blue copper proteins is generally taken as the one with the greatest Cu−S character. In the case of azurin and plastocyanin, it has been shown that the most intense peak is also the one with the largest ^{34}S isotope shift, supporting that assignment (Andrew et al., 1994; Dave et al., 1994; Qiu et al., 1995). That approach is not straightforward for nitrile hydratase because the most intense peak in the spectrum of the high-pH form is not the one with the largest ^{34}S shift. Nonetheless, if we assume that the primary Fe−S vibration in the low-pH form is the one at 393 cm^{-1} (the most intense peak and the one with the largest ^{34}S shift) and in the high-pH form is the one at 445 cm^{-1} (the most intense peak and one of the largest ^{34}S shifts), Badger's rule predicts that the Fe−S bond length shrinks by 0.08 Å. A second approach for blue copper proteins was used by Blair et al. (1985). They used the relative intensities of the peaks in the spectra to calculate a weighted average of the frequencies and used that as representative of the native Cu−S stretch. For nitrile hydratase, the intensity-weighted average of the frequencies in the spectrum of the low-pH form is 373 cm^{-1}, while for the high-pH form, it is 400 cm^{-1}. Here, Badger's rule predicts that the average Fe−S distance shrinks by 0.06 Å. Although neither of these procedures is rigorous, they agree that the Fe−S bond length in the high-pH form of nitrile hydratase is about 0.06−0.08 Å shorter than in the low-pH form. Evidence for a reduction in the Fe−S bond length upon going from pH 7.3 to 9.0 is also available in the EXAFS data (Scarrow et al., 1996).

A shortening of the average Fe−S bond length is consistent with the difference in the EPR spectra of the two forms of nitrile hydratase. Comparison of the EPR spectra predicts an increase in the energy of the d_{xy} orbital, which lies in the plane of the two cysteine ligands, in the high-pH form. Shortening the average Fe−S bond length should give rise to an increase in the energy of that orbital, consistent with the prediction.

Analysis of the Iron−Histidine and Iron-Hydroxide Coordination. The model we propose for the structure of the iron site (Figure 1) predicts coupling between the metal−sulfur and metal−imidazole stretching modes following absorption into the S → M charge transfer band. Consequently, it is possible that some of the features in the 300−500 cm^{-1} region of the resonance Raman spectra reflect modes that involve S−Fe−Im motions. That notion is supported by the observation of significant ^{15}N isotope shifts in most of those features. A simple analysis using an asymmetric linear three-body system as a model (Mohan & Müller, 1972) suggests that the magnitude of the ^{15}N shift in a *trans* S−Fe−ImH system should be approximately half the ^{34}S shift in a peak arising from the symmetric stretching mode.[3] For most of the features in the 300−500 cm^{-1} region, the ^{15}N shift is as large or larger than the ^{34}S shift, suggesting that S−Fe−ImH coupling is not the sole origin of the ^{15}N isotope effects. In one case in particular, the 337 cm^{-1} peak in the spectrum of the low-pH sample shifts −7.1 cm^{-1} in the ^{15}N-labeled sample, though the ^{15}N shift predicted for a two-body Fe−N oscillator is only −6.2 cm^{-1}. Consequently, there must be multiple origins of the ^{15}N shifts, including coupling to motions involving the peptide amide of the cysteines (see above) and the coordinated imidazoles, that result from the uniform labeling of the protein.

The feature at 238 cm^{-1} in the resonance Raman spectrum of the low-pH form is tentatively assigned to have a substantial contribution from an Fe−imidazole stretching mode by analogy to assignments of features found between 254 and 287 cm^{-1} in the spectra of blue copper proteins (Larrabee & Spiro, 1980; Nestor et al., 1984; Woodruff et al., 1984; Blair et al., 1985; Maret et al., 1986; den Blaauwen et al., 1993) and Rieske-type iron−sulfur proteins (Kuila et al., 1992). On the basis of $^{65/63}Cu$ and $^{2/1}H$ isotope effects on the copper−imidazole band in stellacyanin, it was suggested that the imidazole ligand should be treated as a rigid body (Nestor et al., 1984).[4] If we follow that treatment here, exchange of one ^{2}H for ^{1}H in a hypothetical Fe−ImH diatomic oscillator would give rise to a maximum ^{2}H shift of −0.77 cm^{-1} at 238 cm^{-1}. We observe a shift of −1.6

[3] Intuitively, this can be seen as the result of the assumed rigid-body imidazole having approximately twice the mass of the sulfur.

[4] That assumption has been challenged. Isotope shifts in spectra of deoxymyoglobin are better fitted if one assumes the Fe−N unit moves against the rest of the imidazole (Wells et al., 1991).

cm^{-1} in the 238 cm^{-1} feature upon ^2H_2O exchange of the low-pH form of nitrile hydratase. Observation of an unexpectedly large ^2H isotope shift in stellacyanin after exchange into ^2H_2O prompted the suggestion that both the N3 and C2 protons of the histidine were exchangeable in that case (Nestor et al., 1984). The same appears to be true here. Analogously, replacement of two ^{14}N atoms by ^{15}N in a rigid-body imidazole should give rise to a maximum shift of 1.5 cm^{-1} in a two-body Fe−ImH oscillator. We observe a −1.4 cm^{-1} shift in the 238 cm^{-1} band upon uniform labeling with ^{15}N, consistent with this representing an Fe−Im stretch. In the case of the H117G mutant of azurin, coordination of [U-^{15}N]imidazole to the copper led to an approximately 1 cm^{-1} shift in the 284 cm^{-1} band assigned to the Cu−imidazole stretch (Loehr, 1992; Sanders-Loehr, 1993).

The observation of a significant ^{34}S shift in this peak in spectra of the low-pH form of nitrile hydratase suggests mixing of the Fe−S modes in this feature as well. The coincident decreases in ^{34}S shift and resonance enhancement of this peak upon going from pH 7.3 to 9.0 support this idea. Coupling between these modes has a precedent in model studies [Qiu (1994) #63] in which the band at 234 cm^{-1}, assigned by normal mode analysis to a Cu−N(pyrazolyl) stretch, has a contribution nearly as large from the Cu−S mode.

However, the assignment of the 238 cm^{-1} feature in the nitrile hydratase spectra to an iron−imidazole stretch must be considered to be tentative for two reasons. First, the feature appears at substantially lower energy in nitrile hydratase as compared to the blue copper proteins (238 vs 254−287 cm^{-1}), even though the metal−ligand bond lengths are approximately the same [the average Fe−N(O) bond length in the low-pH form of nitrile hydratase is 1.99 Å (Scarrow et al., 1996), whereas in blue copper proteins, the Cu−N bond lengths range from 1.91 to 2.21 Å (Guss & Freeman, 1983; Baker, 1988; Adman et al., 1989; Collyer et al., 1990; Nar et al., 1991; Guss et al., 1992; Redinbo et al., 1993; Fields et al., 1994; Romero et al., 1994)]. Note, however, that in deoxymyoglobin, a high-spin ferrous system, the iron−imidazole stretch is seen at 218 cm^{-1} (Wells et al., 1991) and the Fe−N bond length is 2.1 Å (Takano, 1977). Second, in our samples, the imidazoles are not specifically labeled with ^{15}N, so it is possible the shift in the 238 cm^{-1} peak arises from a different interaction. Note too that there is no requirement that the Fe−imidazole stretch give rise to a resonance-enhanced peak in the Raman spectrum. For example, in Fe^{3+}-substituted liver alcohol dehydrogenase, metmyoglobin, the myoglobin−CO complex, and imidazole-treated Cu^{2+}-substituted liver alcohol dehydrogenase, no evidence of a metal−imidazole stretch is visible in the resonance Raman spectra, though there is independent evidence for coordination of the imidazole to the metal ion (Maret et al., 1986; Wells et al., 1991).

The model in Figure 1 also predicts that coupling between the Fe−S and Fe−O vibrations could contribute to the resonance Raman spectrum. However, we did not detect any significant ^{18}O isotope shifts in resonance Raman spectra of enzyme exchanged into $H_2{}^{18}O$. This negative result is analogous to the result obtained in studies of copper-substituted liver alcohol dehydrogenase, where no ^{18}O isotope effect was seen even though there is evidence for water coordinated to the metal ion (Maret et al., 1986). In both cases, there is no detectable coupling between the M−O vibration and the M−S modes excited in the Raman experiment.

There has been a report of intrinsic nitric oxide ligands to the iron in nitrile hydratase from *Rhodococcus* sp. N-771 (Honda et al., 1992), calling into question the model for the iron site presented in Figure 1. That conclusion was based on observation of an IR peak at 1869 cm^{-1} that shifted 37 cm^{-1} upon growth of the organism on ^{15}N and was thus assigned to an NO stretch. This is unusually high energy for an iron−nitrosyl NO stretch, implying substantial donation from the NO π^* orbital into a bonding Fe−N orbital (Brown et al., 1995), and therefore an unusually strong Fe−NO bond. We saw no corroborating evidence for a feature between 1800 and 2000 cm^{-1} in the resonance Raman spectra of nitrile hydratase.

Several of the bands in the 300−800 cm^{-1} region are candidates for Fe−NO stretching or bending modes because they have substantial ^{15}N isotope shifts. Low-spin Fe(II)−NO complexes[5] show an Fe−NO stretch in the 500−600 cm^{-1} region with a −9 to −15 cm^{-1} ^{15}N isotope shift (Benko & Yu, 1983; Hu & Kincaid, 1991; Lipscomb et al., 1993). In this case, we expect that feature at higher energy, consistent with the strong Fe−NO bond predicted from the unusually high NO stretching frequency (see above). The only peak above 500 cm^{-1} with a large ^{15}N isotope shift is the one assigned to ν_{C-S}. We conclude that there is no evidence to support the existence of NO coordinated to the iron in nitrile hydratase in the resonance Raman data, although the characteristic features may not be resonance-enhanced. We also point out that there is no evidence in the EXAFS data for the predicted very short Fe−NO bond (Scarrow et al., 1996).

Evidence for Hydrogen Bonding to the Iron-Coordinated Cysteines. Several features in the 300−500 cm^{-1} region of the resonance Raman spectra of both the low-pH and high-pH forms of nitrile hydratase show small shifts after exchange of the protein into ^2H_2O. This is a very common phenomenon for both blue copper and iron−sulfur proteins and is generally considered to arise from exchange of protons involved in hydrogen bonding to the metal-coordinated cysteine (Maret et al., 1986; Ainscough et al., 1987; Mino et al., 1987). Crystal structures of metal−sulfur proteins usually show at least one hydrogen bond to every metal-coordinated sulfur (Adman et al., 1975, 1989; Guss & Freeman, 1983; Baker, 1988). The magnitudes of the ^2H shifts in the resonance Raman spectra of blue copper and iron−sulfur proteins are approximately the same as those we are seeing in nitrile hydratase spectra, and it is reasonable to conclude that there are hydrogen bonds to the iron-coordinated cysteine sulfurs.

Structural Interpretation of the Differences between the Low- and High-pH Forms of Nitrile Hydratase. The resonance Raman data suggest that the strength of at least one of the Fe−S bonds is significantly different in the low- and high-pH forms of nitrile hydratase. There is also evidence for the existence of hydrogen bonds to one or both of the metal-coordinated cysteines. It has been suggested

[5] The iron must be formally low-spin ferrous for nitrile hydratase to exhibit an EPR spectrum characteristic of $S = {}^1/_2$ if there is a single NO ligand. Consequently, low-spin ferrous heme−NO complexes are logical models.

by Spiro and colleagues that a difference in the number of hydrogen bonds to the metal coordinated cysteines in plastocyanin and azurin is at least partly responsible for the difference in the Cu−S bond strength in those proteins (Qiu et al., 1995) that is reflected in a shift of intensity in the resonance Raman spectra. In *Alcaligenes denitrificans* azurin, the cysteine sulfur accepts two hydrogen bonds (Nar et al., 1991) and the most intense peak is at 408.6 cm^{-1} (Dave et al., 1993), while in poplar plastocyanin, the cysteine sulfur accepts one hydrogen bond (Guss et al., 1992) and the most intense peak is at 419.9 cm^{-1} (Qiu et al., 1995). It is logical that an additional hydrogen bond would draw off electron density from the sulfur, rendering it less Lewis basic and weakening the metal−sulfur bond. It is difficult to quantify the effect of this difference in hydrogen bonding on the Cu−S distances in the two proteins. A survey of crystallographic results shows a spread of Cu−S bond lengths determined for poplar plastocyanin of 2.07−2.20 Å (Colman et al., 1978; Guss et al., 1992; Fields et al., 1994), with the highest-resolution analysis (1.33 Å) showing 2.07 ± 0.04 Å (Guss et al., 1992). EXAFS analyses yielded a Cu−S bond of 2.09 ± 0.02 Å after multiple determinations (Scott et al., 1982; Penner-Hahn et al., 1989). The crystallographically determined Cu−S bond length in *A. denitrificans* azurin is 2.13 ± 0.05 Å (Norris et al., 1986).

We have estimated the difference in the average metal−sulfur bond length in the low- and high-pH forms of nitrile hydratase to be 0.06−0.08 Å. On the basis of the comparison of azurin and plastocyanin, it is conceivable that loss of a hydrogen bond from one or both metal-coordinated cysteines could give rise to this magnitude of change in Fe−S bond length. This small of a difference in metal−ligand bond length is unlikely to be observed crystallographically and is on the edge of what is significant in the EXAFS analysis. Yet is gives rise to dramatic changes in the resonance Raman and EPR spectra. The fact that the ^2H isotope shifts are comparable in the low- and high-pH forms does not necessarily argue against this model because the magnitudes of the ^2H_2O dependent shifts in the Cu−S features in azurin and plastocyanin are approximately the same, despite crystallographic evidence of differences in the number of hydrogen bonds to the coordinated cysteine sulfur.

Summary. We have presented analyses of resonance Raman spectra of the novel iron−sulfur protein nitrile hydratase, with comparison to previously characterized metal−sulfur proteins. This tool gives detailed information about the cysteine ligands to the metal ion that complements information about the histidine and hydroxide ligands that is available from ENDOR (Jin et al., 1993; Doan et al., 1996). We are in the process of using this battery of very sensitive and powerful probes of the metal site to study the effects of binding of substrates and inhibitors to the enzyme.

REFERENCES

Adman, E. T., Watenpaugh, K. D., & Jensen, L. H. (1975) *Proc. Natl. Acad. Sci. U.S.A 72*, 4854−4858.

Adman, E. T., Turley, S., Bramson, R., Petratos, K., Banner, D., Tsernoglou, D., Beppu, T., & Watanabe, H. (1989) *J. Biol. Chem. 264*, 87−99.

Ainscough, E. W., Bingham, A. G., Brodie, A. M., Ellis, W. R., Gray, H. B., Loehr, T. M., Plowman, J. E., Norris, G. E., & Baker, E. N. (1987) *Biochemistry 26*, 71−82.

Andrew, C. R., Yeom, H., Valentine, J. S., Karlsson, B. G., Bonander, N., Vanpouderoyen, G., Canters, G. W., Loehr, T. M., & Sanders-Loehr, J. (1994) *J. Am. Chem. Soc. 116*, 11489−11498.

Badger, R. M. (1934) *J. Chem. Phys. 2*, 128−131.

Baker, E. N. (1988) *J. Mol. Biol. 203*, 1071−1095.

Benko, B., & Yu, N.-T. (1983) *Proc. Natl. Acad. Sci. U.S.A 80*, 7042−7046.

Bernet, N., Arnaus, A., & Galzy, P. (1990) *Biocatalysis 3*, 259−267.

Bigey, F., Janbon, G., Arnaud, A., & Galzy, P. (1995) *Antonie van Leeuwenhoek 68*, 173−179.

Blair, D. F., Campbell, G. W., Schoonover, J. R., Chan, S. I., Gray, H. B., Malmstrom, B. G., Pecht, I., Swanson, B. I., Woodruff, W. H., Cho, W. K., English, A. M., Fry, H. A., Lum, V., & Norton, K. A. (1985) *J. Am. Chem. Soc. 107*, 5755−5766.

Briand, D., Dubreucq, E., Perrier, V., Grimaud, J., & Galzy, P. (1994) *Microbios 78*, 205−214.

Brown, C. A., Pavlosky, M. A., Westre, T. E., Zhang, Y., Hedman, B., Hodgson, K. O., & Solomon, E. I. (1995) *J. Am. Chem. Soc. 117*, 715−732.

Carrano, C. J., Carrano, M. W., Sharma, K., Backes, G., & Sanders-Loehr, J. (1990) *Inorg. Chem. 29*, 1865−1870.

Chen, L. A., Sharma, P., Legall, J., Mariano, A. M., Teixeira, M., & Xavier, A. V. (1994) *Eur. J. Biochem. 226*, 613−618.

Collyer, C. A., Guss, J. M., Sugimura, Y., Yoshizaki, F., & Freeman, H. C. (1990) *J. Mol. Biol. 211*, 617−632.

Colman, P. M., Freeman, H. C., Guss, J. M., Murata, M., Norris, V. A., Ramshaw, J. A. M., & Venkatappa, M. P. (1978) *Nature 272*, 319−324.

Czernuszewicz, R. S., Kilpatrick, L. K., Koch, S. A., & Spiro, T. G. (1994) *J. Am. Chem. Soc. 116*, 7134−7141.

Dave, B. C., Germanas, J. P., & Czernuszewicz, R. S. (1993) *J. Am. Chem. Soc. 115*, 12175−12176.

Dave, B. C., Czernuszewicz, R. S., Prickril, B. C., & Kurtz, D. M. (1994) *Biochemistry 33*, 3572−3576.

den Blaauwen, T., Hoitink, C. W. G., Canters, G. W., Han, J., Loehr, T. M., & Sanders-Loehr, J. (1993) *Biochemistry 32*, 12455−12464.

Doan, P. E., Nelson, M. J., Jin, H., & Hoffman, B. M. (1996) *J. Am. Chem. Soc.* (in press).

Fields, B. A., Bartsch, H. H., Bartunik, H. D., Cordes, F., Guss, J. M., & Freeman, H. C. (1994) *Acta Crystallogr. D50*, 709−730.

Guss, J. M., & Freeman, H. C. (1983) *J. Mol. Biol. 169*, 521−563.

Guss, J. M., Bartunik, H. D., & Freeman, H. C. (1992) *Acta Crystallogr. B48*, 790−811.

Han, J., Adman, E. T., Beppu, T., Codd, R., Freeman, H. C., Huq, L., Loehr, T. M., & Sanders-Loehr, J. (1991) *Biochemistry 30*, 10904−10913.

Han, S., Czernuszewicz, R. S., & Spiro, T. G. (1989) *J. Am. Chem. Soc. 111*, 3496−3504.

Herschbach, D. R., & Laurik, V. W. (1961) *J. Chem. Phys. 35*, 458−463.

Honda, J., Nagamune, T., Teratani, Y., Hirata, A., Sasabe, H., & Endo, I. (1992) in *Enzyme Engineering XI* (Clark, D. S., & Estell, D. A., Eds.) pp 29−36, New York Academy of Science, New York.

Honda, J., Kandori, H., Okada, T., Nagamune, T., Shichida, Y., Sasabe, H., & Endo, I. (1994) *Biochemistry 33*, 3577−3583.

Hu, S., & Kincaid, J. R. (1991) *J. Am. Chem. Soc. 113*, 9760−9766.

Jin, H., Turner, I. M., Jr., Nelson, M. J., Gurbiel, R. J., Doan, P. E., & Hoffman, B. M. (1993) *J. Am. Chem. Soc. 115*, 5290−5291.

Kuila, D., Schoonover, J. R., Dyer, R. B., Batie, C. J., Ballou, D. P., Fee, J. A., & Woodruff, W. H. (1992) *Biochim. Biophys. Acta 1140*, 175−183.

Larrabee, J. A., & Spiro, T. G. (1980) *J. Am. Chem. Soc. 102*, 4217−4223.

Lipscomb, L. A., Lee, B.-S., & Yu, N.-T. (1993) *Inorg. Chem. 32*, 281−286.

Loehr, T. M. (1992) *J. Raman Spectrosc. 23*, 531−537.

Maret, W., Shiemke, A. K., Wheeler, W. D.; Loehr, T. M., & Sanders-Loehr, J. (1986) *J. Am. Chem. Soc. 108*, 6351−6359.

Mayaux, J.-F., Cerbelaud, E., Soubrier, F., Faucher, D., & Petré, D. (1990) *J. Bacteriol. 172*, 6764−6773.

Mino, Y., Loehr, T. M., Wada, K., Matsubara, H., & Sanders-Loehr, J. (1987) *Biochemistry 26*, 8059−8065.

Mohan, N., & Müller, A. (1972) *J. Mol. Struct. 12*, 275−281.
Nagasawa, T., & Yamada, H. (1989) *Trends Biotechnol. 7*, 153−158.
Nagasawa, T., Ryuno, K., & Yamada, H. (1986) *Biochem. Biophys. Res. Commun. 139*, 1305−1312.
Nagasawa, T., Nanba, H., Ryuno, K., Takeuchi, K., & Yamada, H. (1987) *Eur. J. Biochem. 162*, 691−698.
Nagasawa, T., Takeuchi, K., & Yamada, H. (1988) *Biochem. Biophys. Res. Commun. 155*, 1008−1016.
Nagasawa, T., Takeuchi, K., & Yamada, H. (1991) *Eur. J. Biochem. 196*, 581−589.
Nar, H., Messerschmidt, A., Huber, R., van de Kamp, M., & Canters, G. W. (1991) *J. Mol. Biol. 221*, 765−772.
Nelson, M. J., Jin, H., Turner, I. M., Jr., Grove, G., Scarrow, R. C., Brennan, B. A., & Que, J. L. (1991) *J. Am. Chem. Soc. 113*, 7072−7073.
Nestor, L., Larrabee, J. A., Woolery, G., Reinhammar, B., & Spiro, T. G. (1984) *Biochemistry 23*, 1084−1093.
Norris, G. E., Anderson, B. F., & Baker, E. N. (1986) *J. Am. Chem. Soc. 108*, 2784−2785.
Penner-Hahn, J. E., Murata, M., Hodgson, K. O., & Freeman, H. C. (1989) *Inorg. Chem. 28*, 1826−1832.
Qiu, D., Kilpatrick, L., Kitajima, N., & Spiro, T. G. (1994) *J. Am. Chem. Soc. 116*, 2585−2590.
Qiu, D., Dong, S. L., Ybe, J. A., Hecht, M. H., & Spiro, T. G. (1995) *J. Am. Chem. Soc. 117*, 6443−6446.
Que, L., Jr., & Heistand, R. H. (1979) *J. Am. Chem. Soc. 101*, 2219−2221.
Redinbo, M. R., Cascio, D., Choukair, M. K., Rice, D., Merchant, S., & Yeates, T. O. (1993) *Biochemistry 32*, 10560−10567.
Romero, A., Nar, H., Huber, R., Messerschmidt, A., Kalverda, A. P., Canters, G. W., Durley, R., & Mathews, F. S. (1994) *J. Mol. Biol. 236*, 1196−1211.
Sanders-Loehr, J. (1993) in *Bioinorganic Chemistry of Copper* (Karlin, K. D., & Tyeklár, Z., Eds.) pp 51−63, Chapman & Hall, New York.
Scarrow, R. C., Brennan, B. A., Cummings, J. G., Jin, H., Duong, D. J., Kindt, J. T., & Nelson, M. J. (1996) *Biochemistry 35*, 10078−10088.
Scott, R. A., Hahn, J. E., Doniach, S., Freeman, H. C., & Hodgson, K. O. (1982) *J. Am. Chem. Soc. 104*, 5364−5369.
Spiro, T. G., & Czernuszewicz, R. S. (1995) *Methods Enzymol. 246*, 416−460.
Sugiura, Y., Kuwahara, J., Nagasawa, T., & Yamada, H. (1987) *J. Am. Chem. Soc. 109*, 5848−5850.
Takano, T. (1977) *J. Mol. Biol. 110*, 569−584.
Tavares, P., Ravi, N., Moura, J. J. G., Legall, J., Huang, Y. H., Crouse, B. R., Johnson, M. K., Huynh, B. H., & Moura, I. (1994) *J. Biol. Chem. 269*, 10504−10510.
Taylor, C. P. S. (1977) *Biochim. Biophys. Acta 491*, 137−149.
Urushiyama, A., & Tobari, J. (1990) *Bull. Chem. Soc. Jpn. 63*, 1563−1571.
Wells, A. V., Sage, J. T., Morikis, D., Champion, P. M., Chiu, M. L., & Sligar, S. G. (1991) *J. Am. Chem. Soc. 113*, 9655−9660.
Woodruff, W. H., Norton, K. A., Swanson, B. I., & Fry, H. A. (1984) *Proc. Natl. Acad. Sci. U.S.A. 81*, 1263−1267.

BI960163T